Liquid-Phase Activity Coefficients for Saturated HF/H_2O Mixtures with Vapor-Phase Nonidealities Described by Molecular Simulation

Scott J. Wierzchowski and David A. Kofke*

Department of Chemical Engineering, University at Buffalo, The State University of New York, Buffalo, New York 14260-4200

Isothermal−isobaric Monte Carlo molecular simulations are performed to estimate the vapor-phase fugacity coefficients of hydrogen fluoride and water in their mixtures, covering the full range of composition at experimentally known saturation temperatures and 1 atm pressure. These results are combined with three sets of established experimental data for vapor−liquid coexistence in this system to compute corresponding liquid-phase activity coefficients for each. Application of an integral thermodynamic consistency test shows that the new values of the activity coefficients are greatly improved over previously reported values, which had been computed using an ideal-gas treatment for the vapor phase. The consistency test also gives reason to prefer the data of Munter et al. [*Ind. Eng. Chem.* **1947**, *39*, 427] and Vieweg [*Chem. Tech. (Berlin)* **1963**, *15* (12), 734] in relation to results reported more recently by Miki et al. [*J. Electrochem. Soc.* **1990**, *137* (3), 787], but any such conclusions should be taken only with due consideration to the approximations inherent in the analysis.

Introduction

Mixtures of hydrogen fluoride (HF) and water (H_2O) play an important role in many industrial processes.[1] Much of the practical value of the HF/H_2O solution arises from its aggressive behavior. Thus, the vapor mixture is used for etching in the processing of semiconductors, and the solution is used in pickling of steel. In other instances, the mixture results unintentionally, as a byproduct or through contamination, and it is desired to purify the mixture, perhaps via a dehydration process for maintaining anhydrous HF. For these and other applications, it is helpful to have a comprehensive understanding of the thermodynamics of HF/H_2O mixtures. However, the unusual and difficult nature of this system hinders the development of such a characterization. Its corrosive and hazardous behavior makes even the measurement of solution properties problematic. Moreover, strong hydrogen bonding and other phenomena dominate the thermophysical behavior, and these effects complicate the formulation of a good thermodynamic model for this system. HF behaves as a highly nonideal vapor over a broad range of temperatures and pressures.[2] The associating vapor typically forms a mixture of HF oligomers[3−7] that greatly affect the thermodynamic phase behavior. Many recognize the existence of a HF hexamer at equilibrium[2,5,6,8−13] contributing to the anomalous thermodynamic behavior. Most recently, a study by Suhm[7] indicated a collection of oligomers in the vapor phase. Regardless of the details of this distribution, the significant presence of oligomers in the vapor phase results in considerable deviations from ideal-gas behavior. Several molecular[14−16] and thermodynamic[17−22] models of HF have been developed with these features explicitly in mind, and in some cases have successfully captured many of the anomalous properties of HF. The situation with HF/H_2O mixtures is less advanced, but good efforts are being made.[23−25] Undoubtedly, the HF/H_2O saturated-vapor mixture exhibits nonideal behavior from similar origins, and an inability to model this behavior limits not only the prediction and correlation of thermophysical properties but also the interpretation of experimental data.

In general, experimental measurement of the fugacity (or chemical potential) is performed by putting the system of interest in thermodynamic equilibrium with another system for which the fugacity is known. When the system of interest is a liquid, a common choice for the "calibration" system is a saturated vapor, for which the ideal-gas law or another simple model can give the fugacity. Accordingly, when Miki et al.[26] measured the vapor−liquid equilibrium (VLE) properties of the HF/H_2O mixture at atmospheric pressure, they reported activity coefficients for the liquid by assuming an ideal saturated vapor. The strong nonideality of HF and HF/H_2O vapor gives reason to doubt the validity of these derived results. Indeed, Juwono[24] assessed the activity coefficients through an integral thermodynamic consistency test and observed them to be significantly inconsistent. This observation provides little basis to doubt the quality of the experimental measurements; rather, it points to the inappropriateness of using the ideal-gas model to derive activity coefficients from them. Integral tests provide only a weak check of thermodynamic consistency, but they do present a necessary (albeit insufficient) condition that must be satisfied by any thermodynamic activity coefficient data. Our aim in this work is to improve the analysis of the known experimental data for HF/H_2O VLE to the point where the derived activity coefficients meet at least this weak measure of consistency.

A thermodynamic characterization of the HF/H_2O vapor is needed to obtain accurate activity coefficients for the liquid. Presently available experimental data are insufficient for this purpose. In lieu of experiment, a predictive thermodynamic model could be applied. The most appropriate thermodynamic model[19] is based on

* To whom correspondence should be addressed. Tel.: (716) 645-2911 ×2209. Fax: (716) 645-3822. E-mail: kofke@buffalo.edu.

10.1021/ie030437q CCC: $27.50
Published on Web 12/11/2003

the statistical associating fluid theory, which has recently been applied to HF and H_2O.[25] Our application of this model to the problem of determining liquid-phase activity coefficients[24] has not yielded results that substantially improve the consistency of the derived values, so we do not pursue this approach here. Instead, we consider a characterization based on molecular simulation.

Molecular simulation is a computational means to "measure" the thermophysical properties of a system defined in terms of a mathematical model for the intermolecular interactions.[27,28] In principle, it provides exact results (within some arbitrary precision) for a given molecular model. Such results describe real-system behavior accurately to the extent that the molecular model is a true characterization of the actual molecular behavior. Simulation is especially appealing in relation to traditional engineering models (e.g., equations of state) for its potential to provide prediction of new behavior from limited (or no)[29,30] experimental knowledge of other behavior. In this regard, we have available reasonably good models for pure HF and pure H_2O, and with these models, we can perform simulations of HF/H_2O vapor-phase mixtures to obtain the information needed to derive correct (or improved) liquid-phase activity coefficients from the experimental data.

This paper is organized as follows. The next section describes the theory, models, and methods used for this work. We then provide results, including the fugacity coefficients calculated by the simulations, along with activity coefficients calculated from the simulation data and published experimental results for the HF/H_2O mixture; three different experimental data sets are studied in this manner. Improved consistency of the activity coefficients is demonstrated, and the importance of nonideal vapor effects is shown. We finish with a summary of the accomplishments gained through the study.

Models and Methods

Fugacity Coefficients. Our immediate aim in this work is to apply molecular simulation to calculate the fugacities f_i (or fugacity coefficients ϕ_i defined such that $f_i = Py_i\phi_i$, where P is the pressure and y_i is the mole fraction)[31] of HF and H_2O in a vapor-phase mixture. Isothermal−isobaric ensemble Monte Carlo simulations can be applied for this purpose, selecting state conditions (of temperature and pressure) that correspond to experimental data for the saturated vapor over the full range of composition. The methodology used to measure fugacity coefficients has been previously shown and applied to water. Two variants have been considered, both involving the random "test" insertion of a molecule into the simulation volume to probe the fugacity. In the Widom method,[32] the energy change ΔU is measured accompanying the placement of a "test" HF or H_2O molecule at a random position and orientation within the simulation volume. The observed energy change is used to compute an average that, upon sufficient sampling of configurations of the "real" molecules, yields the fugacity coefficient for the inserted species. The working equation is

$$\phi_i = \frac{1}{\frac{P\beta}{N+1}\langle V \exp(-\beta\Delta U)\rangle} \tag{1}$$

where P is the pressure, N is the number of molecules (of both species) being simulated, $\beta = 1/kT$, where T is the temperature and k is Boltzmann's constant, and V is the volume of the system at the instant the insertion is attempted. The angled brackets indicate an isothermal−isobaric ensemble average, in which sampling of the system volume and all molecular positions and orientations is performed. Upon evaluation of the contribution to the ensemble average, the test molecule is removed from the simulation volume (until the next insertion measurement), and consequently it never affects the configurations sampled by the real molecules.

The Widom method loses accuracy in evaluating vapor-phase fugacity coefficients when applied to strongly associating systems, such as those of interest here. The problem is that large contributions are made to the average by rarely encountered insertion attempts that find the test molecule in a favorable energetic configuration (i.e., hydrogen-bonded) with a real molecule. To remedy this problem, Tripathi and Chapman[33] proposed a variation of the Widom method that uses molecule insertion to measure the chemical potential of the molecule in "monomeric" form. That is, insertions that find the test particle "bonded" to a real molecule have no contribution to or effect on the ensemble average. The working equation is thus

$$\phi_i = \frac{1}{\beta P\left\langle \frac{V}{N_i^{\text{mono}}+1}\exp(-\beta\Delta U^{\text{mono}})\right\rangle} \tag{2}$$

where N^{mono} is the (fluctuating) number of unbonded molecules of the inserted species for the configuration in which the insertion is attempted; the "mono" subscript on ΔU indicates the requirement that the inserted molecule not be bonded to another one. The definition of "bonded" is completely arbitrary, but the method is most effective if the definition coincides with the energetically favorable configurations of a pair of molecules. Additional details are available elsewhere.[33]

The problem with Widom insertion for associating fluids is present also in the basic sampling of the configurations of such a system. The energetics of configurations in which molecules are associated favor their contribution to the ensemble average, but they are not often encountered using simple sampling of configurations. Then, once formed, associated configurations are equally reluctant to come apart. These barriers to association and dissociation lead to poor sampling of the relevant configurations. This effect has a direct consequence on the Tripathi−Chapman fugacity coefficient calculation through the term N^{mono}, which fluctuates as molecules come together or separate. To alleviate the problem, we can apply an association bias algorithm.[34] The biasing forces molecules to associate or dissociate while yielding the correct limiting distribution for the sampled ensemble. The methodology has been described and applied[34,35] elsewhere. The inclusion of a biasing scheme into Monte Carlo simulations to explore molecular configurations will promote proper sampling in this highly associating system.

Activity Coefficients. We define the activity coefficient γ_i for a component i at mole fraction x_i in the mixture by taking a reference as the pure component at the temperature and pressure of the solution, so the

fugacity f_i of the component i is

$$f_i(T,P,x_i) = x_i\gamma_i(T,P,x_i)\, f_i^\circ(T,P) \tag{3}$$

The pure-component fugacity f_i° is evaluated via its equilibrium with its vapor at its saturation pressure $P_i^{sat}(T)$

$$f_i^\circ(T,P) = P_i^{sat}(T)\, \phi_i^{sat}(T,P_i^{sat})\, \Phi \tag{4}$$

where ϕ_i^{sat} is the fugacity coefficient of the pure vapor at saturation and Φ is the Poynting correction. Equality of fugacities between liquid and vapor in equilibrium gives

$$x_i\gamma_i(T,P,x_i)\, P_i^{sat}(T)\, \phi_i^{sat}(T,P^{sat})\, \Phi = y_i P \phi_i(T,P,y_i) \tag{5}$$

where $\phi_i(T,P,y_i)$ is the fugacity coefficient of component i in equilibrium with the solution at T and P.

Miki et al.[26] presented HF/H_2O mixture activity coefficients derived from VLE composition data that they measured. The methodology included an assumption that the saturated-vapor conditions are ideal, corresponding to unit fugacity coefficients in eq 5. The resulting equilibrium condition is then

$$x_i\gamma_i P_i^{sat} = y_i P \tag{6}$$

We use the same composition data and saturated-vapor pressures as those given by experiment, but we measure the fugacity coefficients (of the mixture and pure phases) via molecular simulation, using the methods reviewed in the previous section. Given this information, the activity coefficient γ is easily determined from eq 5.

Consistency Test. The thermodynamic consistency of activity coefficient data can be assessed using methods derived from the Gibbs−Duhem equation. The data we wish to consider are isobaric, and all apply at 1 atm of pressure. They are not isothermal but cover temperatures from 292.65 to 386.85 K. Heat effects are significant for the HF/H_2O system, so we cannot ignore enthalpic contributions in the consistency test. In this case the appropriate equation for an integral consistency test[36,37] is

$$\int_{x_1=0}^{x_1=1}\left[\ln\left(\frac{\gamma_1}{\gamma_2}\right) - \frac{H^E}{RT^2}\frac{dT}{dx_1}\right] dx_1 = 0 \tag{7}$$

where H^E is the temperature- and composition-dependent molar excess enthalpy in the liquid:

$$H^E = H(T,P,x) - \sum_i H_i^\circ(T,P) \tag{8}$$

with H the solution enthalpy and H_i° the molar enthalpy of the pure component i. A plot of the integrand of eq 7 gives a curve with some area above the x axis and some below, and if the data are consistent, these areas will be equal, giving a zero integral. A rule of thumb for determining if the areas can be deemed equal compares the area difference to the total absolute area[36]

$$R = \frac{\text{area above} - \text{area below}}{\text{area above} + \text{area below}} \tag{9}$$

There is no strict requirement on the value of this ratio, but data normally are considered to be inconsistent if this is more than a few percent.[36]

The HF pure-phase enthalpies are calculated from extrapolation of heat capacity data with respect to temperature[38] to saturated HF/H_2O conditions. The H_2O pure-phase enthalpies are calculated from integration of a polynomial fit[39] to the saturated HF/H_2O conditions. The HF/H_2O mixture enthalpies are available from Tyner's enthalpy diagram.[40] This information allows calculation of the excess enthalpy of the saturated liquid for all mixture compositions and temperatures. The derivative dT/dx appearing in eq 7 is obtained from a polynomial fit of the experimental HF/H_2O VLE data. The infinite-dilution value for the HF activity coefficient is easily extrapolated from the given data, but extrapolation of the water activity coefficient at infinite dilution is less straightforward. The data of Miki et al. do not extend to mixtures of water very dilute in HF. To avoid an error-prone extrapolation for this case, we instead apply data from other experimental studies to bridge the gap to the pure-water limit.

The area measure has certain limitations as a thermodynamic consistency test,[31] and a preferred method involves the computation of one of the variables (P, x, y) from the others over the composition range.[41,42] However, this approach requires the introduction of a thermodynamic model for the activity coefficients, which we consider problematic for this system, particularly because the data are not isothermal. The area test is useful in the present circumstances, in that it certainly does identify inconsistency in the activity coefficients derived from the ideal-gas model. For example, the ideal-vapor activity coefficients reported by Miki et al. yield an eq 9 area measure of $R = -0.832$, which clearly fails the test. So, in this regard the area test serves a role as a necessary (albeit insufficient) measure of consistency.[36] Moreover, as shown below, the test also provides a basis for gauging the relative validity of the different data sets currently available.

Potential Models. Many potential models for HF and H_2O have been developed in the literature. Here we explore two models for HF, that of Cournoyer and Jorgensen[43] (CJ84) and the (nonpolarizable) model of Jedlovszky and Vallauri[44] (JVNP). The water models used in our study are well established: TIP3P[45] and SPC/E.[46] Each HF model is characterized through a Lennard-Jones (LJ) term and three point charges corresponding to the F atom, H atom, and a middle charge. The H_2O models also have three point charges (placed on each atom) and a LJ term. We combine the LJ parameters for two models through Lorentz−Berthelot mixing rules and thus arrive at models for the HF/H_2O mixture, of which we study three: TIP3P−CJ84, SPC/E−CJ84, and TIP3P−JVNP. In Table 1, the model parameters are summarized, including LJ parameters, bond angles for H_2O, bond lengths, and charges. The energy of the interaction can then be described by

$$U_{ij} = 4\epsilon_{ij}\left[\left(\frac{\sigma_{ij}}{r_{ij}}\right)^{12} - \left(\frac{\sigma_{ij}}{r_{ij}}\right)^{6}\right] + \sum_{a=1}^{3}\sum_{b=1}^{3}\frac{q_i^a q_j^b e^2}{r_{ij}^{ab}} \tag{10}$$

where r_{ij} denotes the distance between center atoms (oxygen and/or fluorine) and r_{ij}^{ab} is the distance between two charges on different molecules. We note the similarities in the LJ parameters of HF and H_2O. The mixing of the parameters results in a small change for F−O LJ parameters, so it is a reasonable way to combine the unlike-atom parameters.

Table 1. Parameters To Define the Energy Surface for HF and H_2O from Eq 10

model	σ (Å)	ϵ (kcal/mol)	$q(e)$	a_{HOH} (deg)	r_{OH} (Å)
H_2O (TIP3P)	3.1510	0.1520	0.4170	104.95	0.9572
H_2O (SPC/E)	3.1660	0.1550	0.4238	109.47	1.0000

model	σ (Å)	ϵ (kcal/mol)	$q(e)$	r_{FX} (Å)	r_{FH} (Å)
HF (CJ84)	2.9839	0.1510	0.7250	0.1660	0.9170
HF (JVNP)	2.8300	0.1190	0.5920	0.1647	0.9730

Unlike-Interaction Parameters

model	σ (Å)	ϵ (kcal/mol)
CJ84−TIP3P	3.0675	0.1550
JVNP−TIP3P	2.9905	0.1350
CJ84−SPC/E	3.0750	0.1530

Simulation Details. Three different experimental data sets were examined, published by Munter et al.,[47] Vieweg,[48] and Miki et al.,[49] respectively. For each set, isothermal−isobaric Monte Carlo simulations[27,28] were performed for a full range of compositions from pure H_2O to pure HF, at 1 atm of pressure and the experimentally determined saturation temperatures;[26,50,51] additionally pure-phase simulations were performed at each mixture temperature and the experimental saturation pressure of the pure component. The conditions are summarized in Table 2. A total of 500 molecules were used for each simulation. After an initial equilibration period, each simulation sampled at least 2×10^5 cycles, where a cycle consisted of 500 configurations. Insertion averages for the chemical potential were performed after each cycle. Block averages were collected through 5×10^3 cycles, and errors were estimated for each simulation property through the Kolafa method.[52] Fugacity coefficients were calculated as described above. The average volume was computed at each state condition. Both the Tripathi−Chapman insertion method and the association biasing algorithm used a common definition of a monomer, viz., any molecule with no other atom center within 3.75 Å (the fluorine and oxygen atoms act as center atoms).

Results and Discussion

Results are collected in Table 2 and displayed in Figures 1−5. Figure 1 shows ϕ^{sat} for pure HF over the range of temperature for VLE of HF/H_2O mixtures. Experimental data are available for these fugacity coefficients, and these are presented in the figure for comparison. Figure 2 provides results for the pure-HF equation of state over these conditions, presented in terms of the compressibility factor $Z = PV/NkT$ and in comparison with experiment. Data for ϕ^{sat} for pure H_2O have been examined elsewhere.[53] Figure 3 shows ϕ_{HF} in the mixture, and Figure 4 shows ϕ_{H_2O} in the mixture, both based on the experimental data of Miki et al.; these figures are presented also to provide an indication of the sensitivity of the results to the choice of the molecular models and to demonstrate the strengths and weaknesses of the Widom and Tripathi−Chapman methods. Figure 5 shows ϕ_i for the mixture used in the consistency test described above.

Several points are worth making with respect to Figure 1. First, with a fugacity coefficient of order 0.6, pure HF is indeed a nonideal gas. Second, the Tripathi−Chapman methodology provides vastly improved measurements of the fugacity coefficient, particularly at lower temperature. The precision of the results using this technique is excellent. Third, the simulation data are in satisfactory agreement with experiment. The results for ϕ^{sat} using the JVNP and CJ84 potential models bound the experimental data where it is available. Unfortunately, inspection of Figure 2 shows that this good characterization does not carry over to the equation of state. The experimental compressibility factor is as much as 50% less than that given by simulation using either potential model.

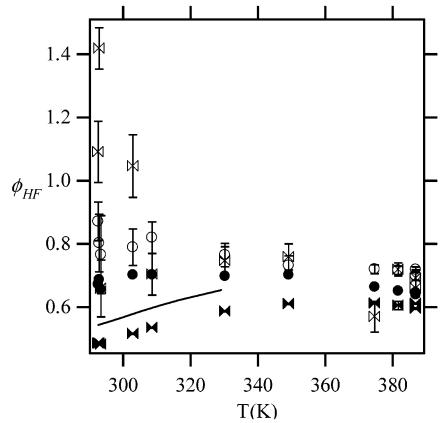

Figure 1. Fugacity coefficient of the saturated vapor of HF as computed by *NPT* Monte Carlo simulation using the JVNP (bow ties) and CJ84 (circles) potential models. Open markers correspond to properties calculated via Widom insertions. Filled markers show properties calculated from the monomer algorithm of Tripathi and Chapman.[33] All visible error bars are associated with the open symbols; errors bars associated with the filled symbols are smaller than the symbol size. The solid line shows experimental properties calculated via $G^R/RT = \ln \phi$, where G^R is taken from Vanderzee and Rodenburg.[2]

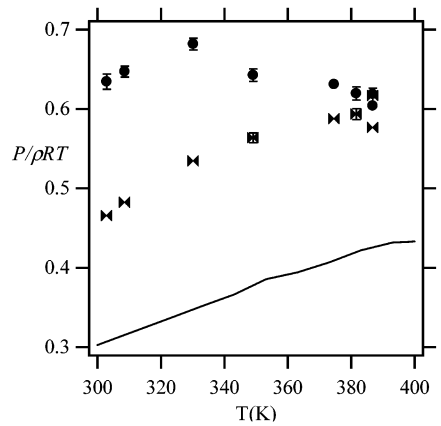

Figure 2. Compressibility factor of the saturated vapor of HF as computed by *NPT* Monte Carlo simulation using the JVNP (bow ties) and CJ84 (circles) potential models. The solid line is experimental data taken from Kao et al.[56]

Figures 3 and 4 present the fugacity coefficients in the mixture and are the key results of this study. Here we find a clarified picture of the nonideal behavior of HF/H_2O mixtures. Figure 3 shows that the fugacity coefficient of HF in the vapor mixture rises from an infinite-dilution value of about 0.2 up to a seemingly ideal value as pure HF is approached. However, just before reaching 100% pure HF, ϕ_{HF} undergoes a precipitous drop to the pure-HF value of about 0.6. This overall behavior is consistent among the three model pairs examined in this study. The Tripathi−Chapman and Widom methods differ, particularly in the approach

Table 2. State Conditions, Number of HF Molecules N_{HF} in Each Simulation, Simulated Fugacity Coefficients, Activity Coefficients, and Heat Effects Needed in the Calculation of the Consistency Test Integrand[a]

T (°C)	vapor wt %	liquid wt %	pure HF P^{sat} (atm)	pure H_2O P^{sat} (atm)	mixture N_{HF}	pure HF ϕ_{HF}^{sat}	pure H_2O $\phi_{H_2O}^{sat}$	mixture ϕ_{HF}	mixture ϕ_{H_2O}	mixture γ_{HF}	mixture γ_{H_2O}	pure HF H (J/mol)	pure H_2O H (J/mol)	mixture H (J/mol)	H^E (J/mol)
(a) Miki et al.[49] State Conditions and Data															
108.5	6.72	24.60	12.650	1.344	30	0.651(2)	0.9462(11)	0.203(8)	0.957(1)	0.0066(2)	0.914(2)	9673	9117	3757	−5487
113.7	51.90	42.00	14.224	1.599	246	0.640(2)	0.9408(5)	0.610(3)	0.626(3)	0.0837(4)	0.349(2)	10254	9557	1473	−8359
113.2	61.05	43.70	14.066	1.573	292	0.646(2)	0.9407(4)	0.725(4)	0.500(2)	0.1136(6)	0.238(1)	10198	9515	1236	−8560
101.5	94.71	54.60	10.757	1.055	470	0.664(2)	0.9532(3)	0.964 (6)	0.159(2)	0.2446(6)	0.0193(2)	8910	8525	−428	−9153
76.0	99.54	66.00	5.686	0.397	497	0.702(2)	0.9723(3)	0.9523(7)	0.0462(43)	0.373(1)	0.00168(15)	6310	6373	−2208	−8542
57.1	99.73	74.10	3.361	0.171	497	0.698(3)	0.9827(2)	0.930(1)	0.0146(19)	0.549(2)	0.00093(12)	4554	4783	−3090	−7708
35.5	99.90	87.50	1.725	0.057	499	0.703(2)	0.9900(5)	0.849(3)	0.00353(70)	0.811(4)	0.00051(10)	2707	2970	−2600	−5344
29.8	99.943	91.60	1.434	0.041	499	0.702(3)	0.9921(2)	0.795(3)	0.00208(40)	0.869(5)	0.00035(7)	2247	2492	−1710	−3979
20.3	99.9911	99.44	1.036	0.024	499	0.656(3)	0.9936(2)	0.646(3)	0.00215(20)	0.956(5)	0.00147(15)	1502	1696	1201	−302
19.8	99.9954	99.76	1.011	0.023	499	0.687(3)	0.9940(2)	0.688(2)	0.00271(30)	0.994(5)	0.00230(26)	1463	1655	1354	−109
19.5	99.9988	99.94	1.000	0.022	499	0.672(4)	0.9943(2)	0.695(3)	0.00168(20)	1.035(8)	0.00151(17)	1440	1629	1441	0
(b) Munter et al.[47] State Conditions and Data															
101.6	0.87	5.47	10.83	1.07	4	0.686(3)	0.9541(8)	0.172(6)	0.957(3)	0.00364(13)	0.980(1)	8920	8534	7207	−1346
102.8	2.03	10.13	11.14	1.11	9	0.669(3)	0.952(2)	0.160(4)	0.959(1)	0.00426(12)	0.978(2)	9050	8635	6220	−2454
106.8	7.06	20.62	12.23	1.28	32	0.656(9)	0.950(1)	0.200(4)	0.955(2)	0.00840(20)	0.911(2)	9485	8974	4345	−4726
108.4	11.63	24.71	12.68	1.34	53	0.648(4)	0.948(2)	0.209(2)	0.960(2)	0.0118(1)	0.872(2)	9662	9109	3743	−5492
110.3	19.41	30.12	13.24	1.43	89	0.662(5)	0.947(1)	0.271(3)	0.926(3)	0.0197(3)	0.780(2)	9873	9270	3022	−6416
111.7	32.82	36.22	13.67	1.50	153	0.653(3)	0.9453(7)	0.372(3)	0.848(3)	0.0377(3)	0.629(3)	10029	9388	2241	−7363
112	34.42	36.82	13.76	1.51	160	0.666(4)	0.944(3)	0.396(4)	0.838(4)	0.0403(4)	0.609(4)	10063	9413	2164	−7473
112.1	36.44	37.63	13.79	1.52	170	0.661(4)	0.944(2)	0.4070(4)	0.803(6)	0.0432(5)	0.571(4)	10074	9422	2060	−7591
112.3	38.17	38.24	13.85	1.52	179	0.653(4)	0.944(1)	0.434(3)	0.797(3)	0.0479(4)	0.554(2)	10096	9439	1980	−7695
112.4	38.28	38.29	13.88	1.53	179	0.648(6)	0.9444(8)	0.437(4)	0.790(5)	0.0485(6)	0.547(3)	10108	9447	1973	−7711
112.1	41.12	39.11	13.79	1.52	193	0.661(4)	0.944(2)	0.465(3)	0.770(5)	0.0537(5)	0.521(3)	10074	9422	1866	−7795
111.4	50.12	42.22	13.57	1.48	237	0.662(4)	0.9472(8)	0.548(5)	0.609(7)	0.0730(9)	0.378(4)	9996	9363	1445	−8169
108.7	65.72	47.01	12.77	1.36	317	0.653(3)	0.951(1)	0.784(4)	0.404(3)	0.134(1)	0.206(2)	9695	9134	759	−8624
101.7	82.61	52.92	10.86	1.07	405	0.672(6)	0.9549(5)	0.934(4)	0.205(4)	0.206(2)	0.0764(15)	8931	8542	−154	−8892
98.9	87.41	54.82	10.16	0.97	431	0.674(4)	0.9580(6)	0.949(3)	0.163(3)	0.229(1)	0.0506(10)	8632	8306	−459	−8935
90.9	92.91	58.62	8.36	0.72	461	0.687(4)	0.964(1)	0.961(1)	0.10(2)	0.275(2)	0.0258(42)	7796	7630	−1076	−8799
86.6	96.21	60.72	7.50	0.61	479	0.688(6)	0.966(1)	0.9641(9)	0.066(28)	0.307(3)	0.0113(48)	7357	7267	−1411	−8731
79	96.29	64.13	6.17	0.44	479	0.704(8)	0.9722(7)	0.951(2)	0.041(17)	0.341(4)	0.0102(42)	6602	6626	−1936	−8547
74.6	98.70	66.22	5.49	0.37	493	0.710(6)	0.9751(8)	0.953(2)	0.029(12)	0.378(3)	0.0032(14)	6175	6256	−2237	−8441
61.6	98.80	72.02	3.83	0.20	493	0.715(4)	0.9812(5)	0.937(3)	0.031(4)	0.483(3)	0.0068(10)	4960	5161	−2919	−7940
45.1	99.30	81.41	2.36	0.10	496	0.699(5)	0.9891(7)	0.901(6)	0.011(2)	0.681(6)	0.0046(8)	3508	3775	−3223	−6785
33.5	99.50	89.01	1.61	0.06	497	0.655(15)	0.9900(5)	0.806(11)	0.0036(10)	0.862(23)	0.0029(8)	2545	2802	−2322	−4898
(c) Vieweg[48] State Conditions and Data															
102.50	2.01	10	11.07	1.10	9	0.681(4)	0.954(1)	0.140(6)	0.959(1)	0.00371(20)	0.985(2)	9017	8610	6247	−2400
106.30	6.78	20	12.09	1.25	31	0.668(4)	0.950(2)	0.184(4)	0.958(2)	0.00763(20)	0.924(2)	9431	8931	4440	−4582
110.30	19.26	30	13.24	1.43	88	0.662(5)	0.946(1)	0.264(3)	0.926(3)	0.0192(3)	0.781(3)	9873	9270	3037	−6401
111.70	43.52	40	13.67	1.50	205	0.653(3)	0.944(1)	0.491(6)	0.731(9)	0.0601(8)	0.489(6)	10029	9388	1747	−7881
104.70	74.25	50	11.65	1.19	361	0.671(4)	0.952(1)	0.865(4)	0.286(3)	0.169(1)	0.134(2)	9256	8796	306	−8708
87.00	90.99	60	7.58	0.62	450	0.704(6)	0.967(1)	0.950(3)	0.0938(2)	0.279(2)	0.03649(7)	7398	7301	−1297	−8654
65.80	98.73	70	4.31	0.25	493	0.752(20)	0.9805(5)	0.945(3)	0.0197(73)	0.424(11)	0.0035(13)	5345	5515	−2712	−8112
47.60	99.91	80	2.54	0.11	499	0.663(5)	0.987(1)	0.899(6)	0.0124(1)	0.681(7)	0.000542(1)	3722	3985	−3263	−7042

[a] Fugacity coefficients are calculated via molecular simulation at corresponding saturated conditions. The CJ84 potential model is used to represent HF; the TIP3P potential model is used to represent H_2O. Heat effects for pure HF are derived from an extrapolation of C_p values to mixture saturated conditions. Heat effects for pure H_2O are calculated from the $C_p(T)$ equation. Heat effects for mixture properties are read from the figure of Tyner.[40] Numbers in parentheses indicate the confidence limits for the last digit in the tabulated value. Confidence limits reflect only the stochastic error in the values of the fugacity coefficients determined by simulation and do not incorporate the experimental error associated with the VLE measurements or error introduced in the estimation of the heat effects.

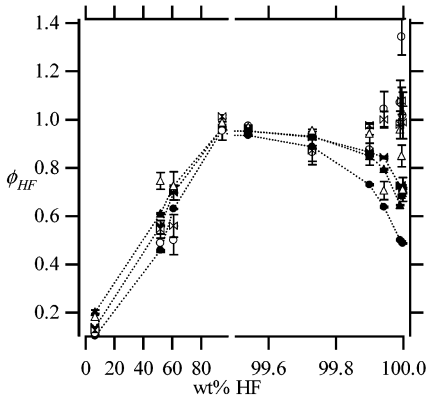

Figure 3. Fugacity coefficient of HF vapor in mixtures with H_2O as computed by *NPT* Monte Carlo simulation at 1 atm and saturation temperatures recorded in Table 2. H_2O/HF potential models used are as follows: SPC/E−CJ84 (bow ties), TIP3P−CJ84 (triangles), and TIP3P−JVNP (circles). Filled markers show results calculated using the monomer algorithm of Tripathi and Chapman methodology, while open markers were computed using simple Widom insertions. Lines join the Tripathi−Chapman results and are given as a guide to the eye. Note the expanded scale for compositions above 99.5 wt % HF.

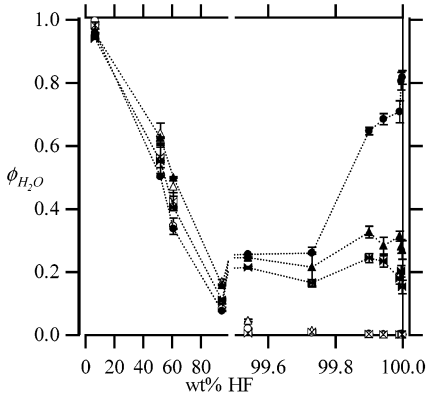

Figure 4. Same as Figure 3 but giving the fugacity coefficient of H_2O.

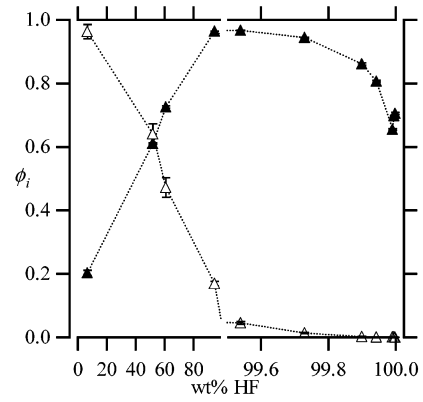

Figure 5. HF/H_2O mixture fugacity coefficients as calculated for saturated temperatures (Table 2) and 1 atm with TIP3P−CJ84 potential models used to analyze activity coefficients (Figure 6). Water fugacity coefficients are designated with open markers. HF fugacity coefficients are designated with closed markers. The figure shows an expanded region above 99.5 wt % HF.

of the pure-HF limit, but it is clear that the Tripathi−Chapman method provides more precise and reliable results for ϕ_{HF}. The reason for this sharp change over a small composition range is exclusively due to the concurrent variation of the saturation temperature in this interval. The saturation temperature drops precipitously here, going from 374.65 to 292.65 K over a vapor composition range of 94.71−100 wt % HF. It should be especially noted that the composition of the simulated system, in fact, changes only slightly across this interval. Canonical-ensemble simulation of a system at the most water-dilute conditions requires a number of HF molecules of order 10^4. The simulations here use only 500 molecules in all cases, so we do not even simulate accurately the composition indicated.

The situation is somewhat different for the water fugacity coefficient (Figure 4). Data for ϕ_{H_2O} drop steadily from nearly ideal values for pure H_2O down to highly nonideal values of order 0.1 upon the approach of pure HF, up to 99.5 wt % HF. Above this value, there is notable deviation between the two chemical potential calculation methods, and this discrepancy persists across mixture potential models. A key consideration in the nearly pure-HF region is again the limitations imposed on the simulation due to finite-size effects. The Tripathi−Chapman method cannot function at such high dilution of water using the relatively small systems employed here. The fraction of H_2O monomers cannot be measured reliably in this situation, where even the fraction of H_2O molecules inaccurately reflects the value of the mixture composition. Results from the Widom insertion methodology are about as good as they are elsewhere: the absolute error is smaller because the fugacity coefficient itself is smaller, but the fractional error is about the same as that at other states. The results show that water is in an extremely nonideal condition, with an infinite-dilution fugacity coefficient that is very close to zero. Water is highly associated with the HF molecules in this vapor. If the Widom method were failing here, it would indicate a too-ideal vapor because its mechanism for failing is missing the contributions from associated configurations. That it indicates a highly nonideal associated vapor gives reason to accept the accuracy of the Widom insertions in this region.

After careful consideration of the various results over all simulation conditions, potential models, and chemical potential methodologies, Figure 5 presents the best estimation of ϕ_{HF} and ϕ_{H_2O} for state conditions of the Miki et al. data set. The required pure vapor ϕ^{sat} for H_2O can be seen elsewhere,[53] and that for HF can be seen in Figure 1.

The implementation of eq 5 allows for calculation of liquid-phase activity coefficients, γ_{HF} and γ_{H_2O}, by combining these simulation results for the vapor-phase fugacity coefficients and the experimental VLE data. The Poynting correction results in a change of at most 1%, and we ignore this factor. The quality of the activity coefficients benefits from the fact that mixture and pure-component ϕ's always appear in a ratio, and consequently limitations in the potential models have some opportunity to cancel. Figure 6 and Table 2 present our estimation from simulation of γ_{HF} and γ_{H_2O} for all experimental data sets, along with (in Figure 6) the values reported by Miki et al. based on an ideal-gas model of the vapor. The ideal-gas results exhibit a range of composition in which both γ_{HF} and γ_{H_2O} have the same slopes, which is a clear failure of a differential thermodynamic consistency test (heat effects notwithstanding). The application of nonideal vapor behavior through ϕ provides an element to the analysis that pushes the activity coefficients toward thermodynamically consis-

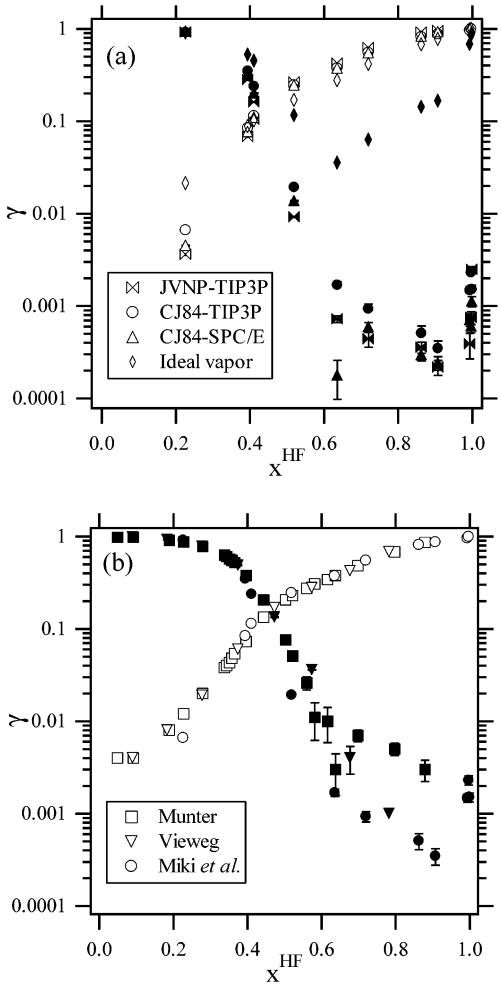

Figure 6. HF/H_2O mixture activity coefficients: (a) using Miki et al.[26] data and HF/H_2O potential models as indicated; (b) using TIP3P−CJ84 potentials with experimental data from sources as indicated. In both figures, open symbols represent HF activity coefficients and filled symbols represent H_2O. Confidence limits indicate the effect of stochastic error in fugacity coefficient calculations and are shown only when larger than the symbol size.

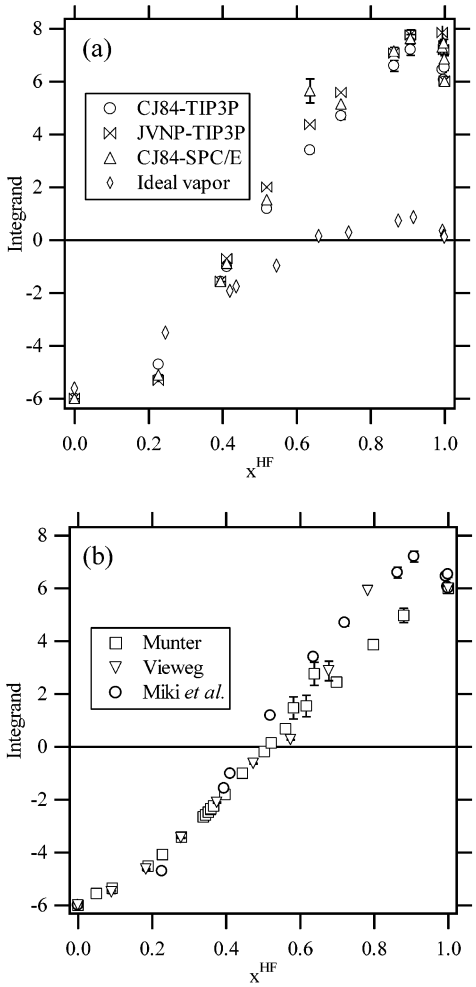

Figure 7. Integrand for the consistency test as calculated from eq 7: (a) using Miki et al.[26] data and HF/H_2O potential models as indicated; (b) using TIP3P−CJ84 potentials with experimental data from sources as indicated.

tent behavior, at least when viewed at this qualitative level. The infinite-dilution behavior reveals extremely nonideal solutions with near-zero activity coefficients (necessitating a log-scale presentation), in contrast to the ideal-gas analysis, which indicates an approach to ideal-solution behavior at infinite dilution with activity coefficients near unity.

The integral consistency test is now applied to the simulation/experiment-derived γ_{HF} and γ_{H_2O}. Figure 7 depicts the comparison between the integrand of eq 7 for all data sets. Further, Table 2 records the information needed to complete a consistency test on them. Experimental data for the Miki et al. set are available only for liquid mixture compositions above 24.6 wt % HF, so to complete the analysis, we must borrow from the other sets from this point to the pure-water composition. The trapezoid rule is applied for numerical integration. Table 3 summarizes values of the heuristic consistency measure (area difference/area sum) so calculated for the combinations of data and models examined here. For the ideal-gas-derived activity coefficients, $R = -0.832$. The consistency test for the Miki et al. data set shows great improvement when applied using the new activity coefficients: the nonideal-vapor heuristic measure is about $R = +0.20$ and insensitive to the choice of the molecular model used to simulate the vapor. Things look even better when we consider the other data sets. Both the Munter et al. and the Vieweg data exhibit a simulation-supplemented consistency measure of less than 0.05. This good value, although not a definitive validation, strongly supports the plausibility of these activity coefficients. Moreover, they give reason to prefer these data sets to that of Miki et al., to the extent that they differ.

Table 3. Consistency Measure Defined by Equation 9 As Derived from the Experimental Data Sets Studied Here, with Vapor-Phase Fugacities Given by Molecular Simulation Using the Potential Models Indicated

experimental data set	molecular models	consistency measure, R
Miki et al.[26]	ideal gas	−0.832
Miki et al.[26]	TIP3P−CJ84	0.142
Miki et al.[26]	TIP3P−JVNP	0.196
Miki et al.[26]	SPCE−CJ84	0.205
Vieweg[48]	TIP3P−CJ84	0.032
Munter et al.[47]	TIP3P−CJ84	0.040

We must recognize that significant approximations are built into this analysis, particularly that due to the molecular models and that associated with grafting of the Munter et al. to the Miki et al. data for mixtures dilute in HF (as well as the trapezoid-rule integration). Further, there exists the possibility that the relatively good performance of the Vieweg and Munter et al. data

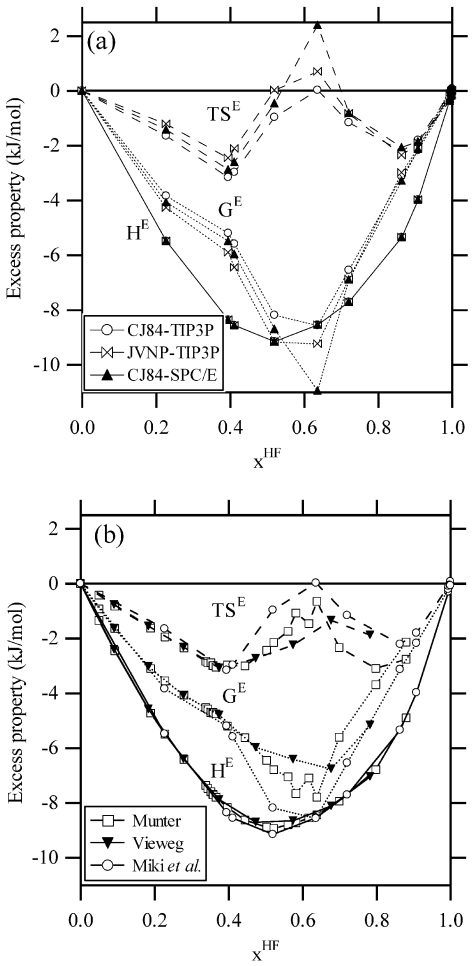

Figure 8. Excess properties of the HF/H_2O mixture. H^E is calculated from eq 8 through use of experimental properties. G^E is calculated from the sum of $RT\ x_i \ln \gamma_i$. TS^E results from $H^E - G^E$. Markers are in (a) using Miki et al.[26] data with TIP3P−CJ84 (crosses), TIP3P−JVNP (bow ties), and SPC/E−CJ84 (solid triangles) and (b) using TIP3P−CJ84 potential with Munter et al. (open squares), Vieweg (solid diamonds), and Miki et al.[26] (crosses).

sets results from a cancellation of error. In this context we should note that a simple linear extrapolation of the Miki et al. integrand across the dilute-HF region intercepts the pure-water limit at a value of about −9.0 (compare to −6.0 when merged with the other data). This added area significantly improves the consistency measure for the Miki et al. data set, giving $R = -0.004$ to +0.050, depending on the vapor-phase molecular model. However, there is no other reason to give preference to such an extrapolation over the data from the other sources.

For completeness, we present excess properties corresponding to the computed activity coefficients. The excess Gibbs free energy is[36,37] $G^E = RT\sum x_i \ln \gamma_i$. The excess enthalpy is given as described above, and the excess entropy is the difference, $TS^E = H^E - G^E$. The (nonisothermal) data are presented in Figure 8. Strong association gives rise to large negative excess enthalpies, and the negative excess entropy indicates a larger degree of ordering, no doubt connected to the association effects also. The excess entropy exhibits a significant change of behavior at about 60% HF, with a peak being apparent. Given that this curve is obtained as the difference in data that are rather noisy, we do not wish to make too much of an issue of this behavior. If correct, however, it is indicative of some interesting structural changes occurring in the saturated liquid through this range of composition. It is notable that the behavior is present in all data sets.

Conclusion

Application of molecular simulation to model saturated-vapor-phase properties of HF/H_2O mixtures has aided in the development of accurate values for the activity coefficients of the corresponding saturated liquid. The improvement is demonstrated through application of an integral consistency test, which shows much more satisfactory results in comparison to previously reported values based on an ideal vapor. The analysis is found to be insensitive to the choice of the molecular model used to describe the intermolecular interactions, and careful attention has been paid to applying the best methodology for evaluation of the vapor-phase fugacity coefficients. These more accurate values of the activity coefficients can be helpful to the development of models for the liquid-phase solution behavior. The nonideal behavior of anhydrous HF is well-known, and the impact of its anomalies on the behavior in mixed systems is highlighted by this work.

This work also provides a pleasing demonstration of the way in which molecular simulation and experiment can be synthesized to provide insights unavailable from either method by itself. The quality of any application of molecular simulation for this type of quantitative analysis always rests with the quality of the molecular model. In this instance, we allowed experiment to provide the description of the highly nonideal, strongly associating liquid, for which details of the molecular model probably have a disproportionate impact on the absolute behavior. Instead, we focus simulation on the nonideal vapor, considering a case in which intermolecular interactions cannot be ignored but where the limitations of the models are not likely to have a highly adverse impact. The advantage is also gained by considering a property in which model inadequacies can cancel to some degree (by taking the ratio of fugacity coefficients). Further, to confirm the model's insensitivity, we have considered how the results vary with the choice of the molecular model.

Certainly a better approach to minimizing the inadequacies of the molecular model is to work with a good model, one that is demonstrated to be capable of providing quantitative agreement with experiment over a broad range of states and for a wide range of properties. Such high-quality models of H_2O and (particularly) HF are not presently available, but efforts to develop such models are progressing well.[54,55] As accurate models emerge for these and other systems, we can expect even more to be able to synthesize simulation and experiment to the good effect demonstrated in this work.

Acknowledgment

We are grateful for several contributions to this research. Financial support was provided by the National Science Foundation (Grant CTS-0076515). Computing facilities were provided by the University at Buffalo Center for Computational Research. We also thank Don Visco for an insightful discussion about the HF/H_2O system.

Literature Cited

(1) Ullmann, F. *Ullmann's Encyclopedia of Industrial Chemistry*; Wiley: New York, 2003.

(2) Vanderzee, C. E.; Rodenburg, W. W. Gas imperfections and thermodynamic excess properties of gaseous hydrogen fluoride. *J. Chem. Thermodyn.* **1970**, *2* (4), 461−478.

(3) Bauer, S. H.; Beach, J. Y.; Simons, J. H. The molecular structure of hydrogen fluoride. *J. Am. Chem. Soc.* **1939**, *61*, 19−24.

(4) Long, R. W.; Hildebrand, J. H.; Morrell, W. E. The polymerization of gaseous hydrogen and deuterium fluorides. *J. Am. Chem. Soc.* **1943**, *65*, 182−187.

(5) Strohmeier, W.; Briegleb, G. The state of association of hydrofluoric acid in the gaseous state. I. New experimental measurements. *Z. Elektrochem.* **1953**, *57*, 662−667.

(6) Simons, J.; Hildebrand, J. H. Density and molecular complexity of gaseous hydrogen fluoride. *J. Am. Chem. Soc.* **1924**, *46*, 2183−2191.

(7) Suhm, M. A. HF vapor. *Ber. Bunsen-Ges. Phys. Chem.* **1995**, *99* (10), 1159−1167.

(8) Maclean, J. N.; Rossotti, F. J. C.; Rossotti, H. S. The self-association of hydrogen fluoride vapor. *J. Inorg. Nucl. Chem.* **1962**, *24*, 1549−1554.

(9) Franck, E. U.; Meyer, F. Hydrogen fluoride. III. Specific heat and association in the gas phase at low pressure. *Z. Elektrochem.* **1959**, *63*, 571−582.

(10) Fredenhagen, K. Physicochemical measurements on hydrofluoric acid. *Z. Anorg. Allg. Chem.* **1933**, *210*, 210−224.

(11) Fredenhagen, K.; Butzke, U. Physicochemical measurements with hydrofluoric acid. (2). *Z. Anorg. Allg. Chem.* **1934**, *218*, 165−168.

(12) Spalthoff, W.; Franck, E. U. Hydrogen fluoride. II. Association in the gas at high pressure. *Z. Elektrochem.* **1957**, *61*, 993−1000.

(13) Briegleb, G.; Strohmeier, W. Association of hydrogen fluoride in the gaseous state. II. *Z. Elektrochem.* **1953**, *57*, 668−674.

(14) Jedlovszky, P.; Mezei, M.; Vallauri, R. Comparison of polarizable and nonpolarizable models of hydrogen fluoride in liquid and supercritical states: A Monte Carlo simulation study. *J. Chem. Phys.* **2001**, *115* (21), 9883−9894.

(15) Cournoyer, M. E.; Jorgensen, W. L. An Improved Intermolecular Potential Function for Simulations of Liquid-Hydrogen Fluoride. *Mol. Phys.* **1984**, *51* (1), 119−132.

(16) Della Valle, R. G.; Gazzillo, D. Towards an effective potential for the monomer, dimer, hexamer, solid, and liquid forms of hydrogen fluoride. *Phys. Rev. B* **1999**, *59* (21), 13699−13706.

(17) Lencka, M.; Anderko, A. Modeling phase equilibria in mixtures containing hydrogen fluoride and halocarbons. *AIChE J.* **1993**, *39*, 533.

(18) Lencka, M.; Anderko, A. Modeling phase equilibria in mixtures containing hydrogen fluoride and halocarbons. *AIChE J.* **1993**, *39* (3), 533−538.

(19) Galindo, A.; Burton, S. J.; Jackson, G.; Visco, D. P.; Kofke, D. A. Improved models for the phase behaviour of hydrogen fluoride: chain and ring aggregates in the SAFT approach and the AEOS model. *Mol. Phys.* **2002**, *100* (14), 2241−2259.

(20) Visco, D. P.; Kofke, D. A.; Singh, R. R. Thermal properties of hydrogen fluoride from EOS+association model. *AIChE J.* **1997**, *43* (9), 2381−2384.

(21) Visco, D. P.; Juwono, E.; Kofke, D. A. Heat effects of hydrogen fluoride from two thermodynamic models. *Int. J. Thermophys.* **1998**, *19* (4), 1111−1120.

(22) Visco, D. P., Jr.; Kofke, D. A. Improved Thermodynamic Equation of State for Hydrogen Fluoride. *Ind. Eng. Chem. Res.* **1999**, *38* (10), 4125−4129.

(23) Anderko, A. Phase equilibria in aqueous systems from an equation of state based on the chemical approach. *Fluid Phase Equilib.* **1991**, *65*, 89−110.

(24) Juwono, E. Engineering modeling of hydrogen fluoride and water mixtures using the statistical associating fluid theory. M.S. Thesis, University at Buffalo, Buffalo, NY, 1998.

(25) Galindo, A.; Whitehead, P. J.; Jackson, G.; Burgess, A. N. Predicting the phase equilibria of mixtures of hydrogen fluoride with water, difluoromethand (HFC-32), and 1,1,1,2-tetrafluoroethane (HFC-134a) using a simplified SAFT approach. *J. Phys. Chem. B* **1997**, *101* (11), 2082−2091.

(26) Miki, N.; Maeno, M.; Maruhashi, K.; Ohmi, T. Vapor−liquid equilibrium of the binary system HF−H_2O extending to extremely anhydrous hydrogen fluoride. *J. Electrochem. Soc.* **1990**, *137* (3), 787−794.

(27) Allen, M. P.; Tildesley, D. J. *Computer Simulation of Liquids*; Clarendon Press: Oxford, U.K., 1987.

(28) Frenkel, D.; Smit, B. *Understanding molecular simulation: from algorithms to applications*, 2nd ed.; Academic Press: San Diego, 2002.

(29) Sum, A. K.; Sandler, S. I. Use of ab initio methods to make phase equilibria predictions using activity coefficient models. *Fluid Phase Equilib.* **1999**, *160*, 375−380.

(30) Sum, A. K.; Sandler, S. I.; Bukowski, R.; Szalewicz, K. Prediction of the phase behavior of acetonitrile and methanol with ab initio pair potentials. II. The mixture. *J. Chem. Phys.* **2002**, *116* (17), 7637−7644.

(31) Prausnitz, J. M.; Lichtenthaler, R. N.; de Azevedo, E. G. *Molecular thermodynamics of fluid-phase equilibria*, 3rd ed.; Prentice Hall PTR: Upper Saddle River, NJ, 1999.

(32) Widom, B. Some topics in the theory of fluids. *J. Chem. Phys.* **1963**, *39* (11), 2808−2812.

(33) Tripathi, S.; Chapman, W. G. An algorithm for calculating the chemical potential in associating and reacting fluids. *Mol. Phys.* **2003**, *101* (8), 1199−1209.

(34) Wierzchowski, S.; Kofke, D. A. A general-purpose biasing scheme for Monte Carlo simulation of associating fluids. *J. Chem. Phys.* **2001**, *114* (20), 8752−8762.

(35) Wierzchowski, S.; Kofke, D. A. UB association bias algorithm applied to the simulation of hydrogen fluoride. *Fluid Phase Equilib.* **2002**, *194*, 249−256.

(36) Sandler, S. I. *Chemical and Engineering Thermodynamics*, 3rd ed.; John Wiley & Sons: New York, 1999.

(37) Prausnitz, J. M.; Lichtenthaler, R. N.; de Azevedo, E. G. *Molecular Thermodynamics of Fluid-Phase Equilibria*; Prentice Hall: Englewood Cliffs, NJ, 1986.

(38) Hu, J.-H.; White, D.; Johnston, H. L. Heat capacity, heat of fusion, and heat of vaporization of hydrogen fluoride. *J. Am. Chem. Soc.* **1953**, *75*, 1232−1236.

(39) Smith, J. M.; Van Ness, H. C.; Abbott, M. M. *Introduction to chemical engineering thermodynamics*, 5th ed.; McGraw-Hill: New York, 1996.

(40) Tyner, M. Enthalpy concentration diagram for hydrogen fluoride water system at one atmosphere. *Chem. Eng. Prog.* **1949**, *45* (No. 1), 49−50.

(41) Van Ness, H. C.; Byer, S. M.; Gibbs, R. E. Vapor−liquid equilibrium. I. Appraisal of data reduction methods. *AIChE J.* **1973**, *19* (2), 238−244.

(42) Abbott, M. M.; Van Ness, H. C. Vapor−liquid equilibrium. III. Data reduction with precise expressions for GE [excess Gibbs function]. *AIChE J.* **1975**, *21* (1), 62−71.

(43) Cournoyer, M. E.; Jorgensen, W. L. An improved intermolecular potential function for simulations of liquid hydrogen fluoride. *Mol. Phys.* **1984**, *51* (1), 119−132.

(44) Jedlovszky, P.; Vallauri, R. Computer simulations of liquid HF by a newly developed polarizable potential model. *J. Chem. Phys.* **1997**, *107* (23), 10166−10176.

(45) Jorgensen, W. L.; Chandrasekhar, J.; Madura, J. D.; Impey, R. W.; Klein, M. L. Comparison of simple potential functions for simulating liquid water. *J. Chem. Phys.* **1983**, *79* (2), 926−935.

(46) Berendsen, H. J. C.; Grigera, J. R.; Straatsma, T. P. The missing term in effective pair potentials. *J. Phys. Chem.* **1987**, *91* (24), 6269−6271.

(47) Munter, P. A.; Aepli, O. T.; Kossatz, R. A. Hydrofluoric acid−water and hydrofluoric acid−hydrofluosilicic acid−water. *Ind. Eng. Chem.* **1947**, *39*, 427−431.

(48) Vieweg, R. Examination of the system HF−H_2O. *Chem. Technol. (Berlin)* **1963**, *15* (12), 734−740.

(49) Miki, N.; Maeno, M.; Maruhashi, K.; Ohmi, T. Vapor−Liquid-Equilibrium of the Binary-System HF−H_2O Extending to Extremely Anhydrous Hydrogen-Fluoride. *J. Electrochem. Soc.* **1990**, *137* (3), 787−790.

(50) Jarry, R. L.; Davis, W., Jr. The vapor pressure, association, and heat of vaporization of hydrogen fluoride. *J. Phys. Chem.* **1953**, *57*, 600−604.

(51) Wagner, W. *Properties of Water and Steam / The Industrial Standard IAPWS−IF97 for the Thermodynamic Properties and Supplementary Equations for Other Properties*; Springer: Berlin, Germany, 1998.

(52) Kolafa, J. Autocorrelations and subseries averages in Monte Carlo simulations. *Mol. Phys.* **1986**, *59* (5), 1035−1042.

(53) Wierzchowski, S.; Kofke, D. A. Fugacity Coefficients of Saturated Water from Molecular Simulation. *J. Phys. Chem. B* **2003**, *107*, 12808−12813.

(54) Wierzchowski, S.; Kofke, D. A., in preparation.

(55) Lisal, M.; Kolafa, J.; Nezbeda, I. An examination of the five-site potential (TIP5P) for water. *J. Chem. Phys.* **2002**, *117* (19), 8892−8897.

(56) Kao, C. P. C.; Paulaitis, M. E.; Sweany, G. A.; Yokozeki, M. An Equation of State Chemical Association Model for Fluorinated Hydrocarbons and HF. *Fluid Phase Equilib.* **1995**, *108* (1−2), 27−46.

Received for review May 19, 2003
Revised manuscript received October 30, 2003
Accepted November 6, 2003
IE030437Q